Leaf-galling phylloxera on grapes reprograms host metabolism and morphology

Paul D. Nabity[a,b], Miranda J. Haus[a], May R. Berenbaum[b,c,1], and Evan H. DeLucia[a,b]

Departments of [a]Plant Biology and [c]Entomology, and [b]Institute of Genomic Biology, University of Illinois at Urbana–Champaign, Urbana, IL 61801

Contributed by May R. Berenbaum, August 30, 2013 (sent for review December 5, 2012)

Endoparasitism by gall-forming insects dramatically alters the plant phenotype by altering growth patterns and modifying plant organs in ways that appear to directly benefit the gall former. Because these morphological and physiological changes are linked to the presence of the insect, the induced phenotype is said to function as an extension of the parasite, albeit by unknown mechanisms. Here we report the gall-forming aphid-like parasite phylloxera, *Daktulosphaira vitifoliae,* induces stomata on the adaxial surface of grape leaves where stomata typically do not occur. We characterized the function of the phylloxera-induced stomata by tracing transport of assimilated carbon. Because induction of stomata suggests a significant manipulation of primary metabolism, we also characterized the gall transcriptome to infer the level of global reconfiguration of primary metabolism and the subsequent changes in downstream secondary metabolism. Phylloxera feeding induced stomata formation in proximity to the insect and promoted the assimilation and importation of carbon into the gall. Gene expression related to water, nutrient, and mineral transport; glycolysis; and fermentation increased in leaf-gall tissues. This shift from an autotrophic to a heterotrophic profile occurred concurrently with decreased gene expression for nonmevalonate and terpenoid synthesis and increased gene expression in shikimate and phenylpropanoid biosynthesis, secondary metabolite systems that alter defense status in grapes. These functional insect-induced stomata thus comprise part of an extended phenotype, whereby *D. vitifoliae* globally reprograms grape leaf development to alter patterns of primary metabolism, nutrient mobilization, and defense investment in favor of the galling habit.

source–sink | *Vitis* | photosynthesis

Parasitism of plants by viruses, bacteria, or insects can result in abnormal tissue growth and altered external morphologies through tumor-like gall formation. Species-specific feeding behaviors of insects determine the type of induced morphologies, which, in addition to the gall itself, can include other structures such as extrafloral nectaries, spines, or trichomes, which may enhance parasite fitness (1–5). These observations are consistent with the concept that gall induction functions as an extension of the parasite phenotype (6). Whereas the mechanisms for host transformations are known for a few bacteria (7, 8), less is known about how insect gall formers initiate and maintain genetic control over plant development.

Gall-forming insects are sedentary and can directly compete for mobilized nutrients with host-plant meristems or developing reproductive structures that act as carbon sinks. Such competition can drive the evolution of the galling habit toward stronger sinks, such as from the leaf edge to the midvein (9) and, among some insect gallers, favors the individual closest to source tissue (10, 11). The sink competition model emphasizes a selective pressure for the galler to become a stronger sink or to manipulate photosynthesis and enhance source strength (i.e., fix more carbon). Stimulation of plant growth through gall-tissue formation requires resource mobilization and thus greater sink demand from the insect and the induced tissues (12, 13); enhancing the source strength to attenuate sink demand is less well documented (but see refs. 14, 15).

The fluid-feeding aphid-like phylloxera *Daktulosphaira vitifoliae* Fitch is a cosmopolitan endoparasite of grapes (*Vitis* spp.) that induces nutrient-enriched galls on leaves or roots. The accidental introduction of phylloxera to Europe and its naïve *Vitis vinifera* in the 1860s devastated grape production and the wine industry there and again threatened viticulture in California in the 1980s with the failure of resistant hybrid rootstocks (16). Phylloxera attack on susceptible cultivated *V. vinifera* may produce hundreds of gall sinks within the plant; however, North American *Vitis* species experience variable levels of leaf galling, depending on species and climatic conditions (17). Unlike other phloem-feeding Aphidomorpha that rely on nitrogen-transaminating bacteria for nutrients, grape phylloxera do not appear to house endosymbionts and feed from the parenchyma (18). Thus, phylloxera likely obtain carbon (C) from starch degradation and nitrogen (N) from amino acid metabolism within the plant. Gall tissues are enriched in starch (19) and amino acids relative to ungalled leaf tissue (20), but how these processes are regulated has been enigmatic.

We report here that stomata, structures that typically benefit the plant by facilitating C fixation and transpiration-driven nutrient/mineral transport, are induced by phylloxera. This unique occurrence allowed us to investigate the manipulation of C fixation and utilization in grape by this aphid-like galler. We hypothesized that if induced stomata increase carbon gain and sink strength for the insect, then additional C fixation should support a greater number of phylloxera, whereas if induced stomata compensate for the effects of gall formation (e.g., C and defense reallocation), then photosynthesis rates may not relate to phylloxera number. We also sequenced the gall transcriptome to determine if large-scale reprogramming of gene expression drives the manifestation of the extended insect phenotype by altering sink/source identity. We showed that phylloxera can induce functional

Significance

Some herbivorous insects induce galls, abnormal structures, in their host plants, benefiting the gall-forming parasite by providing nutritive tissue. The gall-forming insect phylloxera induces stomata, openings through which plants regulate water and CO_2, on the upper surface of grape leaves where they typically do not occur. Carbon uptake and transpiration by induced stomata facilitate nutrient acquisition by gall tissue and phylloxera. Moreover, gall formation reprograms the host-leaf transcriptome to increase transcripts associated with sucrose mobilization and glycolysis and decrease defense-related transcripts. Thus, stomata induction by phylloxera reconfigures leaves to increase carbon gain, to partially offset negative impacts of gall formation.

Author contributions: P.D.N., M.R.B., and E.H.D. designed research; P.D.N. and M.J.H. performed research; P.D.N., M.J.H., M.R.B., and E.H.D. contributed new reagents/analytic tools; P.D.N., M.J.H., M.R.B., and E.H.D. analyzed data; and P.D.N., M.J.H., M.R.B., and E.H.D. wrote the paper.

The authors declare no conflict of interest.

[1]To whom correspondence should be addressed. E-mail: maybe@illinois.edu.

This article contains supporting information online at www.pnas.org/lookup/suppl/doi:10.1073/pnas.1220219110/-/DCSupplemental.

stomata in plants and that this insect transcriptionally reprograms galler-induced tissue beyond primary metabolism to include downstream secondary processes.

Results

Morphological and Functional Characterization of Insect-Induced Stomata. *Vitis* species are hypostomatous, i.e., stomata occur only on the abaxial leaf surface (19, 21–23); however, we observed that stomata appeared on the adaxial leaf surface adjacent to gall tissue after infestation by phylloxera (Fig. 1). For both wild grape and a cultivated hybrid that shares parentage with wild species, the density of adaxial stomata decreased with distance from the developing gall (Table 1, Fig. 1, and Fig. S1). Cross-sections of leaf and gall tissue indicated that adaxial stomata open to intercellular air spaces within the palisade layer and may facilitate CO_2 uptake in the way that abaxial stomata typical of photosynthesizing plants open to diffuse mesophyll (Fig. S2).

Measurements of gas exchange on field- and greenhouse-grown hybrid *Vitis* 'Frontenac' confirmed that stomata on the adaxial leaf surface facilitated CO_2 uptake. In field-grown plants, net CO_2 uptake per unit of leaf area declined in the presence of a single gall, whereas respiration of the galled area increased relative to adjacent ungalled tissue (uptake: $F = 6.89$, df = 1,7, $P = 0.03$; respiration: $F = 20.53$, df = 1,6, $P = 0.004$; Fig. S3). However, the galled leaf area inside the gas exchange cuvette included photosynthetically inactive space (ca.0.1 cm^2 around the adaxial opening of the gall as determined from chlorophyll fluorescence imaging). Accounting for this nonphotosynthetic area, the reduction in photosynthetic leaf area increased CO_2 uptake of galled areas so the difference between galled and ungalled tissue was less significant ($F = 4.58$, df = 1,7, $P = 0.07$). Similarly, respiration per unit dry mass did not differ between galled and ungalled leaf tissue ($t = 0$, df = 12, $P = 0.9$), indicating the increase in respiration occurred due to the increase in gall-induced tissue present. Stomatal conductance (g_s) and transpiration (E) of adaxial leaf sides of galls relative to adjacent ungalled tissues were greater during the day (g_s: $F = 35.56$, df = 1,7, $P < 0.001$; E: $F = 41.28$, df = 1,7, $P < 0.001$) but did not differ at night (g_s: $F = 3.75$, df = 1,6, $P = 0.1$; E: $F = 3.84$, df = 1,6, $P = 0.1$), indicating that adaxial stomata function diurnally as do typical abaxial stomata. The ratio of C uptake to water loss or intrinsic water use efficiency (iWUE) did not differ between galled and ungalled leaves (58 ± 2% vs. 56 ± 4%) but the iWUE calculated for the area of induced adaxial stomata (27 ± 9%) was lower than ungalled tissue ($t = -6.53$, df = 8, $P < 0.001$).

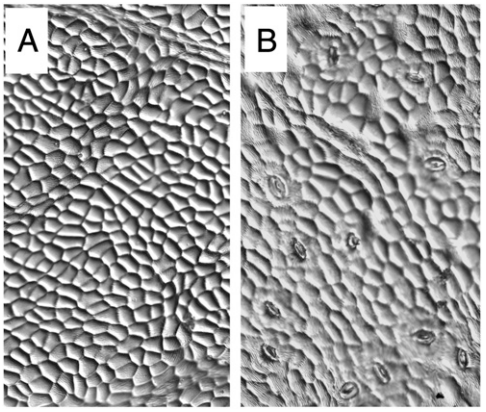

Fig. 1. Epidermal leaf peels show *Vitis* leaves are hypostomatal, having no stomata on the adaxial side (*A*), but gall formation generates stomata in increasing density at closer proximity to the gall (out of picture *Lower Right*; *B*). Abaxial tissue without or adjacent to galls have similar stomata patterning (Table 1).

Table 1. Stomatal index (ratio of stomata to epidermal cells) for *Vitis* species in proximity to gall and in nongalled leaf tissue of galled leaves

		Distance from gall on adaxial side, μm			Nongalled portion of galled leaf	
Species	*n*	0–300	300–600	600–900	Adaxial	Abaxial
V. riparia	5	3.3 ± 0.7a	1.1 ± 0.5b	0.4 ± 0.2b	0 ± 0c	11.0 ± 0.5d
Vitis hybrid	5	1.5 ± 0.3a	0.4 ± 0.1b	0.1 ± 0.1b	0 ± 0c	10.2 ± 0.7d

Stomatal density (SD; number of stomata mm^{-2}) for nongalled areas of galled leaves was 115 ± 8 for *V. riparia* and 270 ± 56 for hybrid *Vitis* 'Frontenac.' Means sharing a common letter within a row do not statistically differ.

To assess how phylloxera feeding and development affected host phenotype, we compared the number of phylloxera to plant physiological and morphological traits. The number of phylloxera within each gall was not correlated with gall size ($R^2 = 0.15$, $F = 2.19$, $P = 0.16$), nightly adaxial CO_2 efflux ($R^2 = 0.04$, $F = 0.5$, $P = 0.5$), or adaxial gross photosynthesis ($R^2 = 0.04$, $F = 0.4$, $P = 0.5$). However, the number of phylloxera within each gall was positively correlated with CO_2 efflux from the adaxial leaf surface (Fig. S4), and this relationship allowed us to estimate the proportion of adaxial CO_2 derived from plant respiration (Fig. S5).

To assess transport dynamics of carbon assimilated by the induced stomata, we labeled CO_2 and traced its movement through the leaf. Leaf photosynthetic capacity determined the uptake of $^{13}CO_2$, whereas respiration demands of gall tissue strongly related to the translocation of fixed C (Fig. S5). Six hours after $^{13}CO_2$ pulses were applied to the abaxial epidermis, the $\delta^{13}C$ value of leaf and gall increased, showing assimilation and transport of C from the adaxial stomata. The $\delta^{13}C$ value of the insect did not increase relative to unlabeled tissues within the same leaf until ≥1 d after labeling when the signal in plant tissues decreased from respiratory loss (1 d $\delta^{13}C$: leaf = 14.2, gall = −6.0, insect = −4.0; 2 d $\delta^{13}C$: leaf = −17.8, gall = −21.3, insect = −0.5). Similarly, $^{13}CO_2$ application to the adaxial surface containing phylloxera-induced stomata increased $\delta^{13}C$ values in the leaf and gall but did not alter $\delta^{13}C$ values in leaf tissue with no insects (Fig. 2). Isotopic enrichment did not alter the percentage of elemental content of any tissues, but ungalled leaf tissue contained more C and N than gall tissues (%C: $F = 259$, df = 3,9, $P < 0.001$; leaf = 45.0 ± 0.4, gall = 43.7 ± 0.2, insect = 57.1 ± 0.4; %N: $F = 121$, df = 3,9, $P < 0.001$; leaf = 3.6 ± 0.2, gall = 2.4 ± 0.2, insect = 7.1 ± 0.1). C uptake and transpiration by induced adaxial stomata facilitated nutrient acquisition by the gall tissue and the phylloxera. Thus, we predicted that pathways related to mobilization of photosynthetic assimilate and nutrients within the xylem would be up-regulated at the transcript level within gall tissue.

Transcriptomic Assessment of the Galling Habit. Examination of the gall transcriptome revealed 2,750 differentially expressed (DE) genes relative to ungalled leaf tissue in 15 functional categories, including photosynthesis, fermentation, and secondary metabolism (Table S1). Expression of genes associated with light harvesting and photosynthetic carbon assimilation strongly decreased, whereas transcripts associated with sucrose mobilization, glycolysis, and fermentation generally increased in gall tissue relative to ungalled leaf tissue (Fig. 3). Transcripts encoding amino acid, oligopeptide, and water transporters also increased (Dataset S1). This concurrent decrease in gene expression related to photosynthetic competency and increase in transport and metabolism processes favors the increase in sink demand initiated and sustained by the insect.

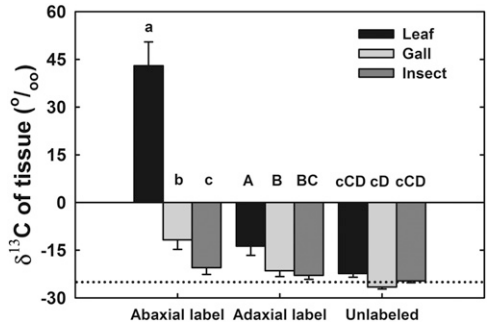

Fig. 2. Postlabeling $\delta^{13}C$ mean value from the corresponding labeled or unlabeled leaf, gall, and insect tissues. Dashed line denotes the $\delta^{13}C$ of unlabeled grape leaves (−24.7 ± 0.8 ‰). Means sharing a common letter do not statistically differ.

Transcripts associated with proteins involved in secondary metabolism showed two distinct patterns (Fig. 3 and Dataset S1). In general, transcripts increased in shikimate and phenylpropanoid biosynthetic pathways, but decreased in nonmevalonate and terpenoid biosynthetic pathways, with a few exceptions, including increases in transcripts for geranyllinalool (GLL) synthase and myrcene synthase, both of which are involved in terpene biosynthesis (Fig. 3 and Dataset S1). Biotic stress-related transcripts for jasmonic acid (JA) and ethylene signaling increased, and the overall gene expression pattern was consistent with salicylic acid (SA) degradation in galls (Fig. 4 and Dataset S1). This defense profile favors insects that are susceptible to SA-based defenses and that may benefit from JA–SA antagonisms existing in many plants (24).

Discussion

Phylloxera feeding on grape leaves induced adaxial stomata that assimilate C and facilitate photosynthate transport to insect-induced tissue. Labeled CO_2 entered leaf stomata in proportion to the photosynthetic capacity, and the respiratory output or metabolic activity of the gall drove acquisition of labeled assimilates. This pathway links adaxial stomata to the sink demand of developing leaf-gall tissue and suggests that phylloxera may benefit from the presence of induced stomata. However, photosynthesis through induced stomata did not relate to insect number, so alternative hypotheses for the adaptive significance of induced stomata may include: (*i*) compensation of plant hosts for insect manipulation of C transport and defense-induced reallocation of C; (*ii*) enhancement of nutrient transport through the xylem to support insect/gall development; or (*iii*) a combination of *i* and *ii*, where inducible stomata benefit both host plant and galler in attenuation of an antagonistic interaction. Galls in other systems (e.g., *Populus*) enhance sink strength to draw resources from ungalled leaves to increase galling aphid progeny numbers, although this ability is diminished in resistant genotypes and may be linked to the capacity for natural plant-bud sink strength (11). Additional evidence in support of hypothesis *ii* is that stomata transport more water than C and evolved to optimize water loss during carbon assimilation (25). We found the iWUE for the induced area with stomata was nearly half the iWUE for ungalled tissues. Although the assimilated C ultimately is consumed by the insect, enhanced nutrient flow driven by transpiration may benefit the insect equally or more than just by providing additional dietary C. This idea gains support from our observation that gall tissues have decreased C yet increased C:N compared with leaf tissue; extra C may not benefit phylloxera that lack endosymbionts

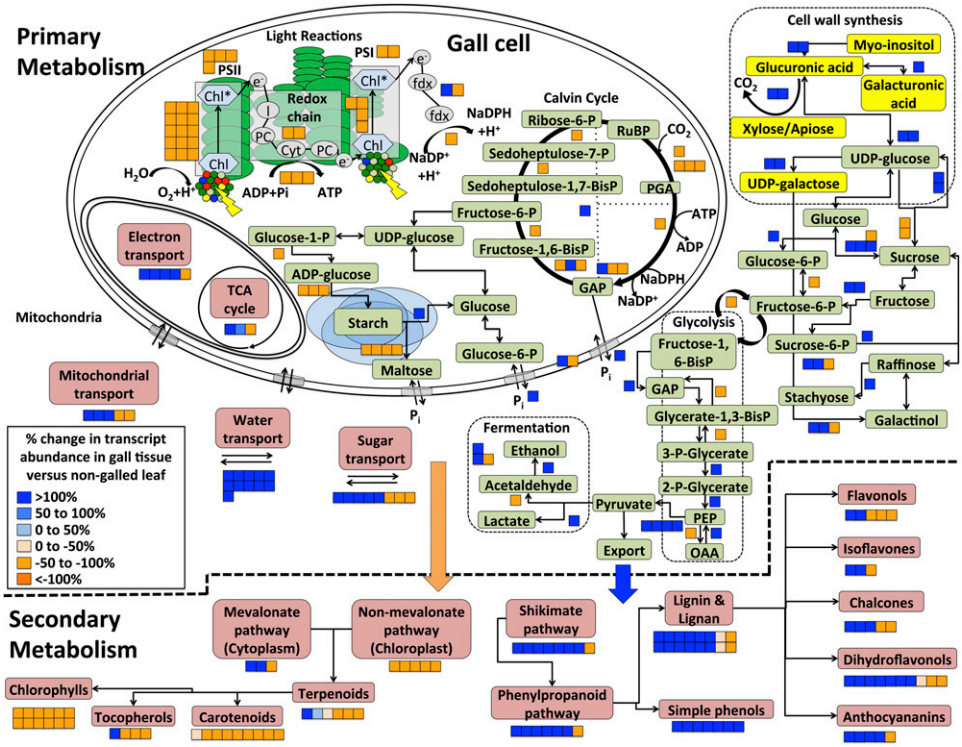

Fig. 3. Graphical representation of the transcriptional shift from autotrophic to heterotrophic metabolism within a gall cell, for inter- and intracellular metabolic processes (glycolysis, fermentation, respiration) and the corresponding downstream transcriptional shift in secondary metabolism. Each orange or blue box represents a unique differentially expressed transcript encoding a protein/enzyme. Green boxes represent metabolites, yellow boxes represent metabolites specifically involved in cell wall synthesis, and pink boxes represent processes. The blue arrow links the up-regulation of glycolysis with corresponding downstream secondary metabolic processes, whereas the orange arrow links the down-regulation of Calvin cycle products with reduced transcript abundance of its corresponding secondary metabolic processes.

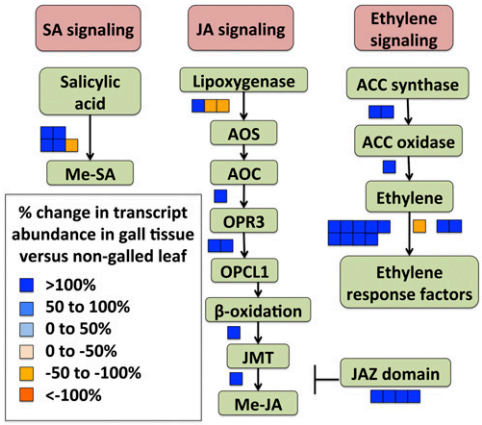

Fig. 4. Graphical representation of the transcriptional shift in biotic defense signaling. Each orange or blue box represents a unique differentially expressed transcript encoding a protein/enzyme. Green boxes represent metabolites and enzymes, whereas pink boxes represent processes.

or rapid excretion found in other Aphidomorpha to mitigate excess C.

Defense hormones (such as JA) may also enhance C translocation to natural plant sinks by increasing invertase activity as a means to increase defense compound synthesis and potentially compensate for herbivore-induced reductions in photosynthesis (26, 27). We observed nearly universal up-regulation of transcripts encoding JA synthesis and up-regulation in vacuolar invertase transcripts (Fig. 4 and Dataset S1) in support of JA-stimulated C transport. Resolving the defense response to phylloxera gall formation may help determine how inducible stomata function within the extended phenotype and whether C, xylem-carried nutrients, or both play a role in the evolution of inducible stomata. Stomata display varying phenotypic plasticity because they optimize the tradeoff of enhancing fitness (i.e., C assimilation and growth) while maintaining plant water status (i.e., transpiration), yet abiotic factors are largely responsible for stomatal patterning and development across plants (28, 29). Induction of stomata by galling insects links biotic and abiotic control over this morphology and suggests that gallers may also regulate the loci that genetically control stomatal patterning and development (30).

Changes in the transcriptome of mature leaf gall tissue suggested that phylloxera manipulate the genes of their grape host to reconfigure its metabolism from an autotrophic to a heterotrophic profile. We observed an overall reduction in gene expression related to photosynthesis but an overall increase in gene expression related to sugar mobilization, glycolysis, and fermentation. Transcripts unique to heterotrophy strongly increased. Expression of genes encoding phosphoglycerate mutase, which converts 3-phosphoglycerate to 2-phosphoglycerate, and enolase, which converts 2-phosphoglycerate to phosphoenolpyruvate, increased relative to expression in ungalled leaf tissue. The enhanced C transport to gall tissue was supported by an increase in the C:N ratio despite decreased C and N content in leaf gall tissue. Previous work found that N content tends to be lower in gall tissue but depends on growth status; faster-growing cells contain higher N (20). Because we sampled mature gall tissue, the growth cycle may have been in the senescent stages. Regardless, we observed a general up-regulation of amino acid and oligopeptide transporters that supports previous findings on amino acid enrichment in galled leaf (20) and root (31) tissue. Amino acid enrichment is expected in sink tissue where phloem unloading of amino acids takes place. This finding is consistent with the lower N content of leaf gall tissue (relative to leaf tissue) because some amino acids decrease (e.g., glutamine and leucine), whereas others substantially increase in leaf gall tissue (e.g., alanine and methionine) (20).

The shift in primary metabolism toward heterotrophic energy production is consistent with the up-regulation of transcripts for cell wall synthesis and the pathway-specific regulation of secondary metabolism. Transcripts for enzymes involved in the biosynthesis of both sugars and phenolics, such as laccases, or those involved in lignin/lignan biosynthesis increased and provide transcriptional support for development of the gall structure. Transcripts encoding shikimate and phenylpropanoid biosynthesis increased, whereas transcripts encoding nonmevalonate biosynthesis and its downstream pathways decreased (Fig. 3). This pattern may be expected in low-oxygen environments within gall tissues (7, 32) where the oxygen-dependent tricarboxylic acid (TCA) cycle is reduced in favor of glycolysis or fermentation. Histological sections of the gall (Fig. S2 and refs. 21 and 22) show that aberrant cell growth produces clustered cells with little air space that may lead to hypoxia. Low-oxygen environments also stimulate ethylene synthesis, which may feed back to inhibit nitrate reductase and contribute to lower N content of tissues. Similar shifts in solutes and transcripts occur in *Agrobacterium tumefaciens* galls (7) and indicate that N is not synthesized in the gall but rather is imported via oligopeptide transporters (33), likely mediated by glycolysis- and phosphoenolpyruvate dephosphorylation-generated ATP. Excess mobile sugars produced during glycolysis may also feed forward to affect synthesis pathways and increase metabolites such as anthocyanin (34) and may explain why some galls appear red in color. We also observed suppression in genes encoding enzymes involved in biosynthesis of other photosynthetic pigments such as carotenoids and chlorophylls, which decrease under phylloxera attack (35), and whose amino acid substrates are reduced in gall tissues (20). Of enzymes related to terpene synthesis, GLL synthase was strongly up-regulated. GLL comprises up to 95% of terpenes found in other sink tissues, such as flowers and berries (36).

Feeding from the parenchyma reduces the need for N-producing symbionts but requires C and N mobilization from the plant, which our transcriptional and physiological data suggest the leaf supplies. Beyond regulating nutritional status, however, phylloxera must also avoid eliciting defenses. Root-feeding phylloxera may induce phenolic accumulation in damaged cells (29), and galls also emit a range of volatiles, including hexanal and hex-2-enal [both lipoxygenase (LOX)-derived volatiles], methyl salicylate, and several volatiles originating from phenylpropanoid and mevalonate biosynthesis (37). Although we examined leaf galls, our transcriptome data are consistent with the synthesis of these metabolites and suggest phylloxera-regulated gene expression within the leaf well beyond C metabolism.

Insect feeding in a variety of plants elicits defenses specific to their feeding mechanism. The few galling insects investigated thus far, a tephritid maggot (*Eurosta solidaginis* Fitch) and a gelechiid caterpillar (*Gnorimoschema gallae-solidaginis* Riley), do not induce JA in their *Solidago* host plants (38), nor does the Hessian fly (*Mayetiola destructor* Say) attacking wheat (*Triticum aestivum* L.) (39). However, we observed a pronounced increase in gene expression for JA (LOX)-defense signaling and a similar up-regulation in SA-carboxyl-methytransferases that degrade SA into methylated SA. This pattern contrasts with the general defense response to Aphidomorpha feeding observed in many other plant species (40) but may indicate that SA defenses are suppressed in favor of phylloxera. Necrotrophic pathogens (e.g., mildews) induce JA signaling (e.g., refs. 41, 42) so phylloxera may induce defense signaling to prevent competition with mildews for plant resources. Foliar JA application decreased fecundity of root-feeding insects (43), although methylated JA also induces stilbenes, anthocyanins, and piceids (31, 44) and can increase SA in grape (45). The interactions of these hormones make it difficult to extend the parasite phenotype to include

manipulation of defense signaling and metabolism, at least until additional data on the metabolite pools are available. Given that methylated SA emitted by plants compromises the ability of some parasitoids to locate hosts (46) but enhances this ability in some predatory mites (47), the role for SA in phylloxera–grape interactions is unclear.

Here we describe the occurrence of functional galler-induced stomata and link the physiological and genomic regulation of the gall to galler-derived sink strength. The formation of stomata as part of an extended phenotype facilitates nutrient transport and thereby may reduce interspecific competition that can occur between galling insects and natural plant sinks (10) or intraspecific competition that results from insects colonizing the same leaf (11). In view of our genomic data on the processes regulated during the maintenance of galler-induced tissues, parsing out the role of nutrient acquisition in relationship to gall ontogeny in this system should not only shed light on the evolution of the galling habit and the adaptive significance of induced morphologies, it may also be of value to viticulturists selecting for traits in host genotypes that increase resistance to phylloxera. The ability of this gall-forming insect to manipulate its host by inducing the formation of stomata, anatomical structures that balance carbon gain with water loss while facilitating nutrient transport, allows this parasite to reduce the negative effects of herbivory and increase the compatibility between a parasite and its host.

Materials and Methods

Plant and Insect Material. Vines of *Vitis riparia* Michx. and the cultivated interspecific hybrid 'Frontenac' that shares parentage with wild grapes (National Grape Registry, http://ngr.ucdavis.edu) were grown in a greenhouse to characterize stomata under relatively constant environmental conditions. *Vitis* 'Frontenac' were also grown under field conditions for a single season to assess stomatal function under typical vineyard conditions. Greenhouse vines were cloned from field cuttings from a single vine growing at the University of Illinois Fruit Research Farms, whereas *V. riparia* plants were propagated from seed (Prairie Moon Nursery). Both species were grown in 10-L pots filled with soilless media (LC1 Sunshine; SunGro Horticulture). Vines were provided with monthly applications of 10% NPK (wt/vol) and watered when necessary. Local *D. vitifoliae* taken from *Vitis* 'Frontenac' leaves from a nearby vineyard were colonized on vines, and both plants and insects were maintained in a greenhouse with supplemental lighting (28:22 ± 2 °C, 16:8 L:D). Field plots of *Vitis* 'Frontenac' vines (1X vines; Double A Vineyards) were planted before spring bud break, watered with 200 ppm N amendment for 1 mo to encourage vegetative growth, and watered thereafter when needed. Local *D. vitifoliae* were collected from infested vineyards and allowed to colonize vines (in May). All histology, gas exchange, and transcriptomic experiments used *Vitis* 'Frontenac.'

Histology and Imaging. One galled and one uninfested leaf from each of five phylloxera-infested greenhouse-grown vines were harvested to determine the occurrence and structure of leaves with induced adaxial stomata. Epidermal peels (Fig. 1) were prepared by painting cellulose acetate (nail varnish) onto leaf surfaces and then plating the imprint for microscopy. To determine stomatal number, impressions of the galled and ungalled surfaces of galled and ungalled leaves were made with dental resin (President Plus; Coltene/Whaledent, Inc.). Digital renderings of the impression surface were profiled using optical topometry (Nanofocus μsurf explorer; Nanofocus) (Fig. S1). Cell number was counted using the Motif Operator (μSoft Analysis Premium software; Nanofocus). Intact leaf and gall tissues were harvested from vines and immediately submerged in 10% neutral buffered formalin for >1 d, serially dehydrated in ethanol, and embedded in paraffin. Tissue cross-sections (Fig. S2) were made with a microtome (Leica RM2255; Leica Microsystems, Inc.) and then stained with hematoxylin and eosin to delineate cellular structure following standard protocols at the Core Facilities Histology laboratory in the Institute for Genomic Biology, University of Illinois at Urbana–Champaign (UIUC).

Gas Exchange. To determine how the galling habit affects leaf photosynthesis, gas exchange was measured on second-generation galls of similar size from field-grown vines using a portable infrared gas analyzer. Leaves with one gall (n = 10) from unique vines were identified, and daytime CO_2 uptake and nighttime respiration were measured on a portion of the leaf containing the gall and an adjacent ungalled leaf area. Gas exchange at steady state was measured from both leaf surfaces with a 6-cm^2 cuvette (LI6400 IRGA; Licor) at saturating light (25 ± 2 °C, ~50% relative humidity, RH). Subsequently, the sample manifold chamber was sealed with tape and the leaf was inverted in the cuvette to measure one-sided leaf gas exchange from the adaxial surface only while illuminating the abaxial leaf surface. Field measurements were completed within 1 d and repeated the following day on a different cohort of leaves (in June).

CO_2 Labeling. To determine the contribution of adaxial CO_2 influx into galls, greenhouse-grown vines were used to pulse adaxial or abaxial leaf sides with ^{13}C-enriched CO_2. Enriched CO_2 was applied to each leaf surface with a gas exchange system modified for one-sided leaf gas exchange as described, and the sample and reference gas lines were redirected to include airflow through an adjacent 50-mL vial. Leaves (n = 4) were dark adapted (>20 min) to determine abaxial (plant) or adaxial (plant plus insect) respiration and then light-adapted to reach steady state (photosynthetically active radiation = 1,500 $\mu mol \cdot m^{-2} \cdot s^{-1}$, 29 ± 1 °C, RH ~60%). Once leaves were light adapted, 1 mL of 5% (vol/vol) acetic acid in water was injected into the 50-mL vial containing 20 mg of ^{13}C sodium carbonate (IconIsotopes). This released a pulse of ~800 $\mu mol \cdot m^{-2} \cdot s^{-1}$ labeled CO_2 that lasted in the gas exchange system for approximately 4 min. Subsequent pulses of decreasing concentrations were applied with additional 1-mL injections after the previous pulse disappeared and conditions returned to steady state. Each leaf side was labeled with four pulses over 10 min.

We harvested labeled leaves after 6 h because preliminary labeling experiments indicated $^{13}CO_2$ had infiltrated all tissues. One or 2 d after labeling, leaf and gall tissue declined to δ^{13}C values similar to unlabeled leaves, whereas insect δ^{13}C values increased, suggesting the labeled CO_2 was respired out of leaf tissue but accumulated in the insect through feeding. Insect, gall, and leaf tissues from labeled and adjacent unlabeled areas on the same leaf were separated by tissue type. Leaves were divided further into two tissue types: tissue within a 4-mm diameter circle centered on the gall where the stomata occur and remaining leaf tissue lacking adaxial stomata.

Tissues exposed to $^{13}CO_2$ were separated by type, insects and eggs were counted, and all tissues were oven dried at 70 °C. Tissues were weighed, ground to powder, and analyzed with an Elemental Combustion System (model 4010; Costech Analytical Technologies) coupled to a Delta V isotope ratio mass spectrometer (ThermoFisher Scientific).

Data Analysis. Gas exchange parameters and δ^{13}C values of tissues within the same leaf were blocked by machine (LI-6400) for field measurements and analyzed by repeated measures ANOVA (Proc Mixed 9.1; SAS Institute). Elemental content was log transformed before analysis to correct for nonnormality. Regression analyses were conducted by linear regression (Proc Reg; SAS Institute). A Fisher's exact test (Proc Freq; SAS Institute) was used to assess if functional categories assigned by Mapman (48) for transcripts were significantly different relative to the overall gall expression patterns.

RNA Extraction and Sequencing. To assess the transcriptome of mature sinks, galls containing phylloxera of reproductive age and undamaged leaves of similar age were harvested from separate leaves of unique vines. Each damage type was collected from a unique vine and pooled (10 leaves or galls per vine) for a total of three pools (from three vines) per damage type. Tissues were flash frozen in liquid N_2 and stored at −80 °C. Insects were removed from gall tissues before RNA extraction. Total RNA was isolated from frozen tissues using Spectrum Plant Total RNA kit (Sigma-Aldrich). RNA quality and quantity were determined by spectrophotometry (Nanodrop 1000; ThermoFisher Scientific) and a denaturing agarose gel with ethidium bromide staining. Construction of RNA-Seq libraries and sequencing on the Illumina HiSeq2000 instrument were carried out at the W. M. Keck Center for Comparative and Functional Genomics, UIUC. One microgram of DNase-treated total RNA per sample was used to prepare individually barcoded RNAseq libraries with the TruSeq RNA Sample Prep kit (Illumina). Libraries were pooled in equimolar concentration and each pool was sequenced on one lane on a HiSeq2000 for 100 cycles using Version 2 chemistry according to the manufacturer's protocols (Illumina). Thus, three unique read libraries were generated for each damage type and then demultiplexed using Casava 1.7.

Bioinformatics. Reads were aligned to the *V. vinifera* transcriptome (Version 12x; Phytozome Version 7, Joint Genome Institute) by modifying a conservative RNA-Seq read assessment (49). Briefly, raw reads were aligned to the reference transcriptome using two mapping programs for comparison, Novoalign (as in ref. 49) and CLC Genomic Workbench (CLC Bio). A minimum total read count for each tissue was implemented (min = 50) and then differential expression between galled and ungalled leaf tissue was

analyzed for each mapping, using two discrete probability distribution-based methods, DESeq (50) and edgeR (51). DESeq calculates differential expression with estimated variance and size factor normalized data, whereas edgeR tests differential expression using empirical Bayes estimation with exact tests; both tests rely upon the negative binomial distribution as is appropriate for count data. Differentially expressed genes ($P < 0.05$) were combined from each analysis to generate a single gene list. These differentially expressed genes were then merged with *Arabidopsis thaliana* TAIR v9 identifiers. Fold changes from unique *V. vinifera* transcripts that mapped onto duplicate *A. thaliana* genes were averaged, and the remaining genes were placed into functional categories based on the Mapman visualization toolkit (48). Modified pathways (Figs. 3 and 4) were redrawn from the resulting data. This process was repeated by varying minimum total read counts (5, 25, 50), resulting in similar overall expression patterns; however, we only report gene expression that had a minimum count of 50. Our combined list of differentially expressed genes resulted in 4,038 genes, of which 337 did not map to *Arabidopsis* gene IDs and 951 were duplicates. The *V. vinifera* transcript IDs (12x; Phytozome Version 7) and their corresponding *Arabidopsis* IDs (TAIR Version 9) are listed in Dataset S1.

ACKNOWLEDGMENTS. We thank Dawn and Joe Taylor (Sleepy Creek Vineyards) for access to their vines and Sharon Gray, Anna Locke, Cody Markelz, Noah Whiteman, Jack Schultz, Thomas Whitham, and members of E.H.D.'s laboratory for insightful comments on an earlier draft of this paper. This work was supported in part by US Department of Energy Grant DE-FG02-04ER63489 and by US Department of Agriculture Grant 2002-02723.

1. Price PW (1987) Adaptive nature of insect galls. *Environ Entomol* 16(1):15–24.
2. Waring GL, Price PW (1989) Parasitoid pressure and the radiation of a gallforming group (Cecidomyiidae: *Asphondylia* spp.) on creosote bush (*Larrea tridentata*). *Oecologia* 79(3):293–299.
3. Stone GN, Schonrogge K, Atkinson RJ, Bellido D, Pujade-Villar J (2002) The population biology of oak gall wasps (Hymenoptera: Cynipidae). *Annu Rev Entomol* 47:633–668.
4. Wool D (2004) Galling aphids: Specialization, biological complexity, and variation. *Annu Rev Entomol* 49:175–192.
5. Raman A, Schaefer CW (2005) *Biology, Ecology, and Evolution of Gall-Inducing Arthropods*, ed Withers TM (Science Publishers, Plymouth, UK), Vol 1.
6. Stone GN, Schonrogge K (2003) The adaptive significance of insect gall morphology. *Trends Ecol Evol* 18:512–522.
7. Deeken R, et al. (2006) An integrated view of gene expression and solute profiles of *Arabidopsis* tumors: A genome-wide approach. *Plant Cell* 18(12):3617–3634.
8. Stes E, Vandeputte OM, El Jaziri M, Holsters M, Vereecke D (2011) A successful bacterial coup d'état: How *Rhodococcus fascians* redirects plant development. *Annu Rev Phytopathol* 49:69–86.
9. Inbar M, Wink M, Wool D (2004) The evolution of host plant manipulation by insects: Molecular and ecological evidence from gall-forming aphids on *Pistacia*. *Mol Phylogenet Evol* 32(2):504–511.
10. Larson KC, Whitham TG (1997) Competition between gall aphids and natural plant sinks: Plant architecture affects resistance to galling. *Oecologia* 109(4):575–582.
11. Compson ZG, Larson KC, Zinkgraf MS, Whitham TG (2011) A genetic basis for the manipulation of sink-source relationships by the galling aphid *Pemphigus batae*. *Oecologia* 167(3):711–721.
12. Allison SD, Schultz JC (2005) Biochemical responses of chestnut oak to a galling cynipid. *J Chem Ecol* 31(1):151–166.
13. Rehill BJ, Schultz JC (2003) Enhanced invertase activities in the galls of *Hormaphis hamamelidis*. *J Chem Ecol* 29(12):2703–2720.
14. Fay PA, Hartnett DC, Knapp AK (1993) Increased photosynthesis and water potentials in *Silphium integrifolium* galled by cynipid wasps. *Oecologia* 93(1):114–120.
15. Dorchin N, Cramer MD, Hoffmann JH (2006) Photosynthesis and sink activity of wasp-induced galls in *Acacia pycnantha*. *Ecology* 87(7):1781–1791.
16. Granett J, Walker MA, Kocsis L, Omer AD (2001) Biology and management of grape phylloxera. *Annu Rev Entomol* 46:387–412.
17. Downie DA, Granett J, Fisher JR (2000) Distribution and abundance of leaf galling and foliar sexual morphs of grape phylloxera (Hemiptera: Phylloxeridae) and *Vitis* species in the central and eastern United States. *Environ Entomol* 29(5):979–986.
18. Vorwerk S, Martinez-Torres D, Forneck A (2007) *Pantoea agglomerans*-associated bacteria in grape phylloxera (*Daktulosphaira vitifoliae* Fitch). *Agric For Entomol* 9(1):57–64.
19. Witiak SM (2006) Hormonal and molecular investigations of phylloxera leaf gall development. PhD thesis (Pennsylvania State Univ, University Park, PA).
20. Warick RP, Hildebrandt AC (1966) Free amino acid contents of stem and phylloxera gall tissue cultures of grape. *Plant Physiol* 41(4):573–578.
21. Rosen HR (1916) The development of the *Phylloxera vastatrix* leaf gall. *Am J Bot* 3(7):337–360.
22. Sterling C (1952) Ontogeny of the phylloxera gall of grape leaf. *Am J Bot* 39(1):6–15.
23. Pratt C (1974) Vegetative anatomy of cultivated grapes: A review. *Am J Enol Vitic* 25(3):131–150.
24. Thaler JS, Humphrey PT, Whiteman NK (2012) Evolution of jasmonate and salicylate signal crosstalk. *Trends Plant Sci* 17(5):260–270.
25. Peterson KM, Rychel AL, Torii KU (2010) Out of the mouths of plants: The molecular basis of the evolution and diversity of stomatal development. *Plant Cell* 22(2): 296–306.
26. Arnold TM, Schultz JC (2002) Induced sink strength as a prerequisite for induced tannin biosynthesis in developing leaves of *Populus*. *Oecologia* 130(4):585–593.
27. Arnold TM, Appel HM, Schultz JC (2012) Is polyphenol induction simply a result of altered carbon and nitrogen accumulation? *Plant Signal Behav* 7(11):1498–1500.
28. Woodward FI (1987) Stomatal numbers are sensitive to increases in CO_2 from pre-industrial levels. *Nature* 327:617–618.
29. Casson SA, Hetherington AM (2010) Environmental regulation of stomatal development. *Curr Opin Plant Biol* 13(1):90–95.
30. Hancock AM, et al. (2011) Adaptation to climate across the *Arabidopsis thaliana* genome. *Science* 334(6052):83–86.
31. Kellow AV, Sedgley M, Van Heeswijck R (2004) Interaction between *Vitis vinifera* and grape phylloxera: Changes in root tissue during nodosity formation. *Ann Bot (Lond)* 93(5):581–590.
32. Haiden SA, Hoffmann JH, Cramer MD (2012) Benefits of photosynthesis for insects in galls. *Oecologia* 170(4):987–997.
33. Cao J, Huang J, Yang Y, Hu X (2011) Analyses of the oligopeptide transporter gene family in poplar and grape. *BMC Genomics* 12:465.
34. Belhadj A, et al. (2008) Effect of methyl jasmonate in combination with carbohydrates on gene expression of PR proteins, stilbene and anthocyanin accumulation in grapevine cell cultures. *Plant Physiol Biochem* 46(4):493–499.
35. Blanchfield AL, Robinson SA, Renzullo LJ, Powell KS (2006) Phylloxera-infested grapevines have reduced chlorophyll and increased photoprotective pigment content: Can leaf pigment composition aid pest detection? *Funct Plant Biol* 33(5):507–514.
36. Martin DM, et al. (2009) The bouquet of grapevine (Vitis vinifera L. cv. Cabernet Sauvignon) flowers arises from the biosynthesis of sesquiterpene volatiles in pollen grains. *Proc Natl Acad Sci USA* 106(17):7245–7250.
37. Lawo NC, Weingart GJ, Schuhmacher R, Forneck A (2011) The volatile metabolome of grapevine roots: First insights into the metabolic response upon phylloxera attack. *Plant Physiol Biochem* 49(9):1059–1063.
38. Tooker JF, DeMoraes CM (2007) Feeding by Hessian fly [*Mayetiola destructor* (Say)] larvae does not induce plant indirect defences. *Ecol Entomol* 32(2):153–161.
39. Tooker JF, De Moraes CM (2008) Gall insects and indirect plant defenses: A case of active manipulation? *Plant Signal Behav* 3(7):503–504.
40. Walling LL (2008) Avoiding effective defenses: Strategies employed by phloem-feeding insects. *Plant Physiol* 146(3):859–866.
41. Hamiduzzaman MM, Jakab G, Barnavon L, Neuhaus JM, Mauch-Mani B (2005) beta-Aminobutyric acid-induced resistance against downy mildew in grapevine acts through the potentiation of callose formation and jasmonic acid signaling. *Mol Plant Microbe Interact* 18(8):819–829.
42. Trouvelot S, et al. (2008) A beta-1,3 glucan sulfate induces resistance in grapevine against Plasmopara viticola through priming of defense responses, including HR-like cell death. *Mol Plant Microbe Interact* 21(2):232–243.
43. Omer AD, Thaler JS, Granett J, Karban R (2000) Jasmonic acid induced resistance in grapevines to a root and leaf feeder. *J Econ Entomol* 93(3):840–845.
44. Faurie B, Cluzet S, Mérillon JM (2009) Implication of signaling pathways involving calcium, phosphorylation and active oxygen species in methyl jasmonate-induced defense responses in grapevine cell cultures. *J Plant Physiol* 166(17):1863–1877.
45. Repka V, Fischerova I, Silharova K (2004) Methyl jasmonate is a potent elicitor of multiple defense responses in grapevine leaves and cell suspension cultures. *Biol Plant* 48(2):273–283.
46. Snoeren TAL, et al. (2010) The herbivore-induced plant volatile methyl salicylate negatively affects attraction of the parasitoid *Diadegma semiclausum*. *J Chem Ecol* 36(5):479–489.
47. De Boer JG, Dicke M (2004) The role of methyl salicylate in prey searching behavior of the predatory mite *phytoseiulus persimilis*. *J Chem Ecol* 30(2):255–271.
48. Thimm O, et al. (2004) MAPMAN: A user-driven tool to display genomics data sets onto diagrams of metabolic pathways and other biological processes. *Plant J* 37(6): 914–939.
49. Yendrek CR, Ainsworth EA, Thimmapuram J (2012) The bench scientists guide to statistical differential expression analysis of digital gene expression data. *Bioinformatics* 26:139–140.
50. Anders S, Huber W (2010) Differential expression analysis for sequence count data. *Genome Biol* 11(10):R106.
51. Robinson MD, McCarthy DJ, Smyth GK (2010) edgeR: A Bioconductor package for differential expression analysis of digital gene expression data. *Bioinformatics* 26(1):139–140.

Supporting Information

Nabity et al. 10.1073/pnas.1220219110

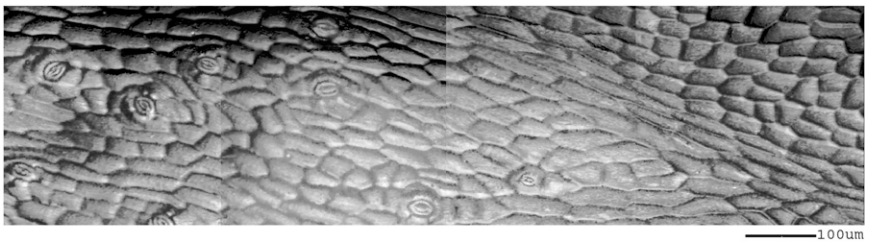

Fig. S1. Composite image of epidermal cells visualized using optical topometry reveals a gradient of adaxial stomata on *Vitis* 'Frontenac' leaves extending outward from a gall (out of picture, far *Left*).

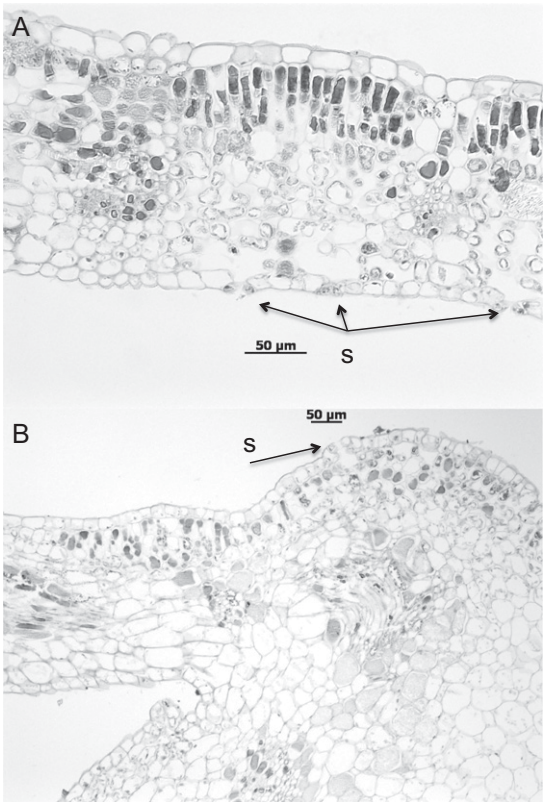

Fig. S2. Cross-sections for *Vitis* 'Frontenac' tissue that is undamaged (*A*) and with developed gall tissue (*B*). Stomata (S) typically form on the abaxial leaf side (*A*) but gall formation generates adaxial stomata. (Scale bar, 50 µm.)

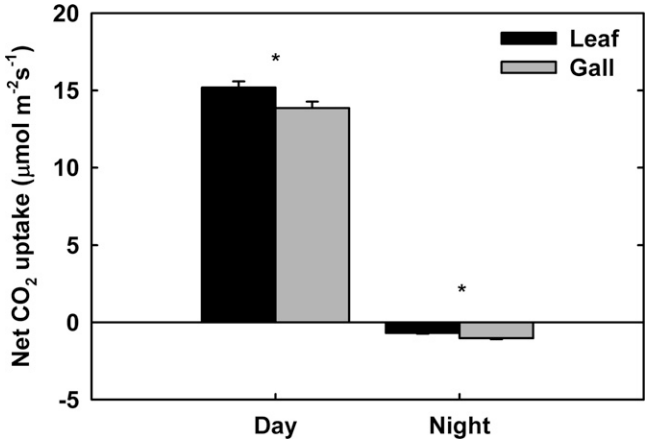

Fig. S3. Whole leaf net CO_2 uptake during the day (positive) and night (negative) of field-grown galled and nongalled adjacent leaf tissue. Fluxes include insect and plant respiration. *Significant differences between tissue types at each time assessed.

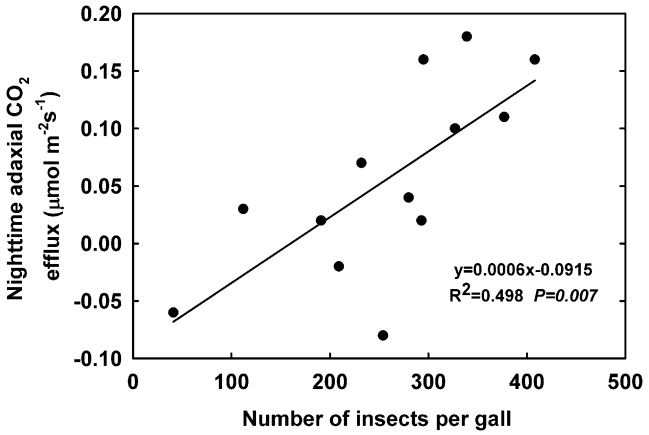

Fig. S4. Nighttime adaxial CO_2 efflux related to the number of insects and eggs within the gall.

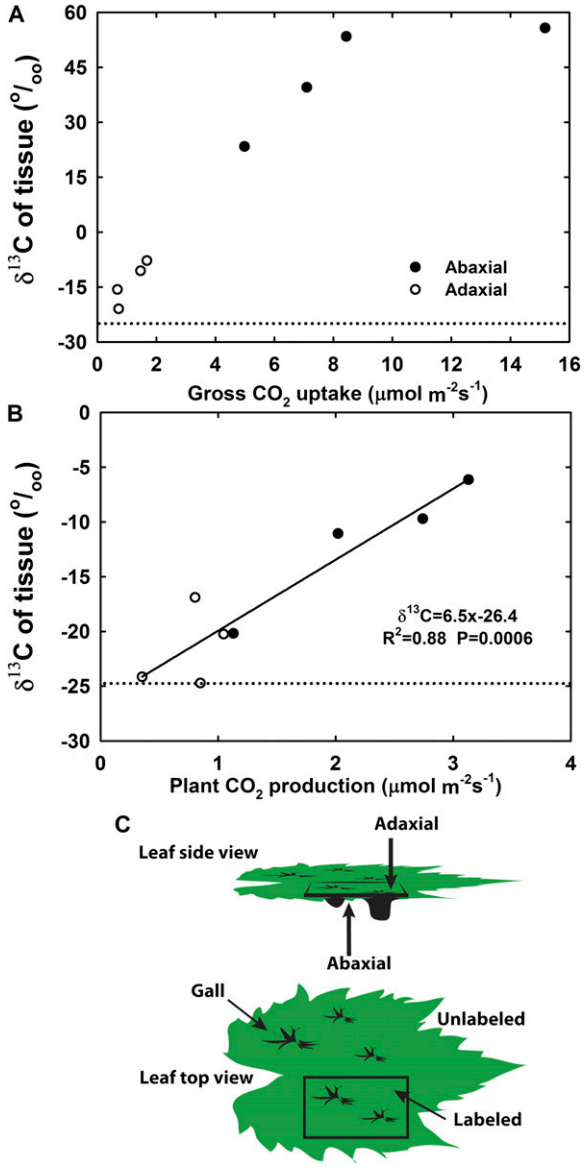

Fig. S5. Postlabeling $\delta^{13}C$ values of leaf tissue related to abaxial or adaxial CO_2 uptake (*A*), abaxial- or adaxial-labeled gall tissue related to its corresponding abaxial or adaxial CO_2 efflux (*B*), and a graphical depiction of leaf sides and where label was applied (*C*). Dashed lines denote the $\delta^{13}C$ of unlabeled grape leaves (−24.7 ± 0.8‰). CO_2 flux from adaxial side was adjusted to remove insect respiration (*Materials and Methods*).

Table S1. Genes and coverage for each functional category adopted from Mapman

Categories	Total genes	DE genes	% coverage
Fermentation	12	6	50
Secondary metabolism	210	99	47
Photosynthesis	136	63	46
Cell wall	219	90	41
Stress	410	151	37
Miscellaneous	660	233	35
Metal handling	44	15	34
Hormone metabolism	272	91	33
Transport	578	177	31
Signaling	707	205	29
Not assigned	4,062	640	16
RNA	1,554	235	15
Protein	1,832	261	14
DNA	320	38	12
Mitochondrial electron transport/ATP synthesis	89	5	6

Mapman categories that were not significantly represented included: amino acid metabolism, biodegradation of xenobiotics, C1-metabolism, cell, cofactor and vitamin metabolism, development, gluconeogenesis/glyoxylate cycle, glycolysis, lipid metabolism, major carbohydrate metabolism, minor carbohydrate metabolism, *N*-metabolism, nucleotide metabolism, oxidative pentose phosphate pathway, polyamine metabolism, redox, sulphur-assimilation, TCA/organelle, transformation, and tetrapyrrole synthesis. DE, differentially expressed.

Other Supporting Information Files

Dataset S1 (XLSX)